

AJP

ISSN : 0971 - 3093

Vol 24, No 12, December, 2015

**ASIAN
JOURNAL OF PHYSICS**

An International Quarterly Research Journal



ap

ANITAPUBLICATIONS

FF-43, 1st Floor, Mangal Bazar, Laxmi Nagar, Delhi-110 092, India

B O : 2, Pasha Court, Williamsville, New York-14221-1776, USA



Large size, high resolution three-dimensional display based on projector array

Xinzhu Sang¹, Binbin Yan¹, Peng Wang¹, Xin Gao¹, and Gang-Ding Peng²

¹State Key Laboratory of Information Photonics and Optical Communications, Beijing University of Posts and Telecommunications, P.O.Box 72, Beijing 100876, China

²Photonics & Optical Communications, University of New South Wales, Sydney 2052, NSW, Australia

Dedicated to Prof Joseph Shamir

To realize high resolution 3D video display without the need of wearing glasses, a huge amount of 3D spatial information is normally required. For a 3D display with smooth motion parallax similar to the holographic stereogram, the size of the virtual viewing slit should be smaller than the pupil size of eye at the largest viewing distance. To achieve high resolution and minimize 3D information necessary for eyes in order to relax requirements on display devices and reduce processing time, two glass-free 3D display systems with rear and front projection are presented. The systems are based on the space multiplexing with a micro-projector array and specially designed 3D diffuse screens with the size about $1.8 \text{ m} \times 1.2 \text{ m}$. The displayed clear depths are larger than 1.5 m. The flexibility in terms of digitized recording and 3D diffuse screen based reconstruction relieves the limitations of conventional 3D display technologies, and fully continuous, natural 3D display is realized. Good aberration suppression and low cross talk have been achieved in both proposed display systems. © Anita Publications. All rights reserved.

Keywords: Parallax, High resolution, 3D video display, Large size, Projector array

1 Introduction

In recent years, the three-dimensional (3D) display which can provide natural scenes and natural-like 3D simulation environments has increasingly drawn interests. To simulate the natural 3D vision, both binocular parallax and motion parallax are required. Normally, it requires a huge amount of spatial information to increase the number of views and to provide smooth motion parallax for natural 3D display similar to real life. However, various tradeoffs for dynamic 3D displays exist, such as number of view points, color, motion parallax, resolution and so on. Volume displays realize 3D images made up of light spots arranged in 3D space by optical scanning based on mechanical components, but they cannot provide a fully convincing 3D experience because of their limited color reproduction and lack of occlusions. Holography is a real 3D image recording and display method that has been considered the ideal method for 3D display. However, it is difficult to realize high quality real-time holographic 3D display in the near future, due to the performance deficiencies on the available spatial light modulator and the significant computational power. The ideal natural 3D display should present the same image quality and viewing conditions as we experience from our surrounding environment. For conventional stereoscopic displays, 3D images do not change while viewers move their heads because only two images for two eyes are displayed. The lack of motion parallax reduces the presence of 3D images and causes visual fatigue. Multiview display provides discontinuous motion parallax because the stereo image pair does not change until the eye moves into the adjacent viewing zone, which reduces the presence and realism effects of 3D images. It is important for the natural 3D display to increase the number of views and provide smooth motion parallax.

A time multiplexed 3D display with the use of a fast digital micro-mirror device based projector and an optical wedge was developed [1]. Combining a high-frame-rate color projector with a flat light field scanning screen, a floating 360-degree light field 3D display was presented [2]. Recently, we demonstrated a large size 3D display based on a holographic functional screen and a projector array with 64 micro-projectors [3, 4], which could deliver natural 3D video display. Holographic stereogram [5] can be used to display

Corresponding author

e-mail: xzsang@bupt.edu.cn (Xinzhu Sang)

a description of 3D discrete images or a set of 3D data points, such as computer aided design 3D model, a topographic-derived image, a number of captured serial images. A given image is visible only through a single virtual viewing slit, which is typically narrower than the pupil diameter of eye. Different images are visible through each virtual viewing slit. With a series of stereo pair images, one can perceive a 3D image with continuous motion parallax. Here, we demonstrate two glasses-free rear and front projection 3D display systems with smooth motion parallax based on the space multiplexing with the micro-projector array and the special designed 3D diffuse screens.

2 Rear projection 3D display with holographic functional screen

The 3D information can be recovered by creating the light field with beams with the relative directions and intensities same as the light originated from a 3D object or scene, which is the base of our display method. Figure 1 shows a schematic configuration of our 3D pickup and display system mainly made up of a video server, an optimally designed CCD camera array, and a projector array in specifically arranged configuration behind the holographic functional screen. We use 64 color CCD cameras to pick up the information of 3D object at different view angles, and 64 color projectors to display the full color 3D space information of the object through the planar holographic functional screen with the size of $(1.8 \times 1.3) \text{ m}^2$. Optical axes of all cameras in the array converge to a common point R. The light beams from projectors with their optical axes converging to a common point R' are projected onto the holographic functional screen at various angles, which are determined by the geometry of the camera array. The magnification depends on the ratio between the geometry sizes of projector and camera arrays. Each camera is individually connected to a PCI card plugged into the video server. The video server is used to capture the images at 64 different view angles through the CCD camera array, correct image distortions, synchronize the image frames, and control the projector array to emit them onto the holographic functional screen. The precise synchronization is essential for real-time 3D display.

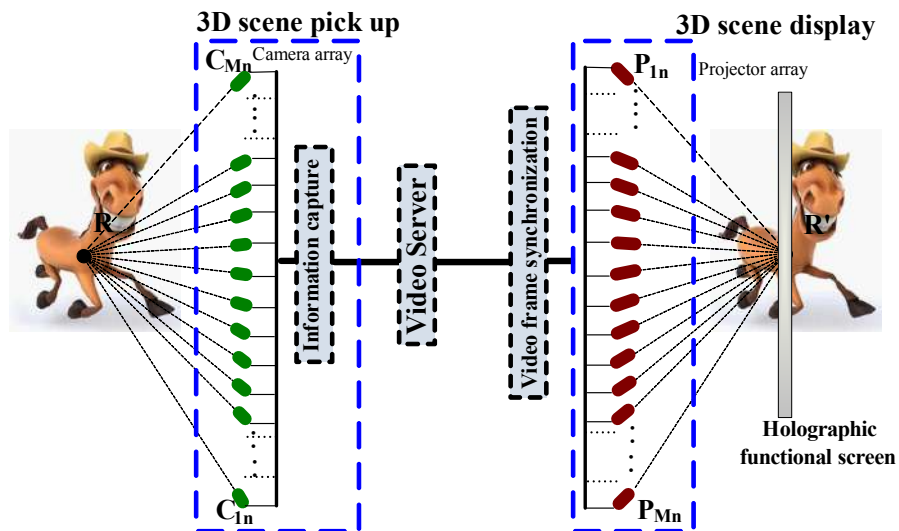


Fig 1. Schematic configuration for the real-time 3D display system

All the projectors illuminate every point on the holographic functional screen. The point of the holographic functional screen emits multiple light beams of various intensities and colors in different directions in a controlled way, as if they were emitted from the point of the real 3D object at a fixed

spatial position. The light beams are generated through projectors arranged in a specific geometry, and the holographic functional screen makes the necessary optical transformation to regulate these beams into a 3D scene. All projectors contribute to each 3D scene view without sharp boundary between views. So the display provides continuous and smooth change at different view areas.



Fig 2. Professor Tung H. Jeong with the large-than-life 3D display [3]

This system exhibits a total horizontal view angle of 45° with uniform brightness and larger than 1 m clear depth. The picture of 3D portrait is displayed along with the real person as shown in Fig 2, where 64 images captured at different view angles are stored in the video server. We can see that the size of the 3D image is larger than that of the real person. The displayed 3D image is very similar to the computer-generated hologram synthesized from multiple angular viewpoints [6], but the 3D display can easily realize large size, high brightness and update without the limitations of the recording material. To compare them, the pictures of the computer-generated hologram and the 3D image in the display system with the same image data are shown in Fig 3. Figure 4 presents the pictures of a 3D portrait taken at two different positions.

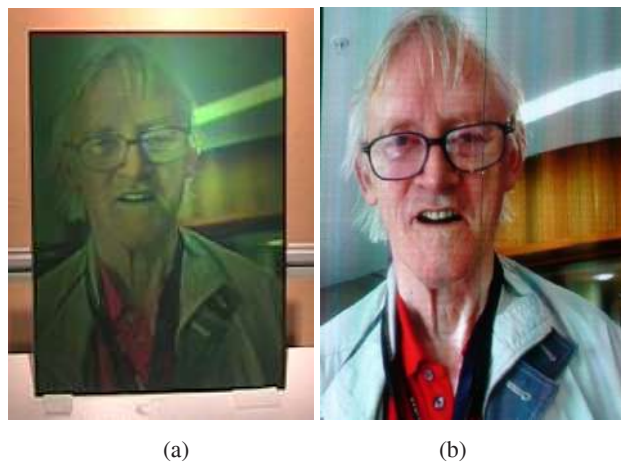


Fig 3. Pictures of (a) the computer-generated hologram and (b) the 3D display in the experiment with the same image data [3].



Fig 4. Pictures of a 3D portrait taken at different positions

3 Frontal projection 3D display

In the 3D display system based on the frontal projection diffuse screen, the arrangement of projector array is based on the light-field distribution in the viewing plane [6]. Figure 5 illustrates the light-field distribution with a single projector in the viewing plane. The diffuse screen is placed in the focal plane of lenticular diffusing sheet.

As shown in Fig 5(a), the light from the projector is focused on the front surface of the diffuse screen with the lenticular sheet, and then it is diffused to pass through the lenticular sheet in the second time. The emergent light is refracted to different directions and formed periodical viewpoints containing the same content. T represents the width of the viewing zones, and W_1 , W_2 are widths of the same viewpoint in DVZ and the adjacent viewing zones, respectively. The lens cell of the traditional lenticular sheet is cylindrical lens. The vertical light stripes represent the same view point in different viewing zones, which are distributed in the viewing plane periodically, as shown in the Fig 5(b). In the same way, other projectors in the projector array also form corresponding periodical vertical stripes representing different viewpoints. Every viewing zone consists of these different vertical stripes. Different parallax images projected on the lenticular sheet are encoded to form a synthetic 3D image.

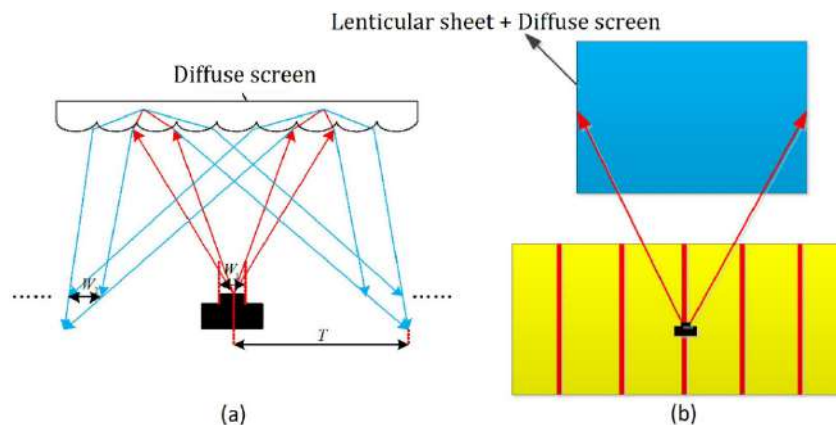


Fig 5. The light-field distribution with a single projector (a) The light path of single projector (b) The distribution of light-field with a single projector

Monte Carlo Non-Sequential Ray tracing arithmetic is used to simulate the light-field distribution in the viewing plane. A projector is placed in the middle position of one meter away in front of the diffusing screen. Figure 6 shows that the width of vertical stripes in MVZ is reduced with increasing ROC. Based on the above analysis, increasing ROC or decreasing aperture can suppress aberration. Two lenticular sheets with different parameters are used in the experiment. A projector is placed in the middle position of three meters away in front of the lenticular sheet. The parameters are shown in Table 1. P , r , d represent the aperture, ROC and thickness of the lenticular sheet, respectively.

Table 1. Parameters of the cylindrical lenticular sheet

P (mm)	r (mm)	d (mm)	L (mm)	Size (m ²)
1.5	5	8	3000	1.9×1.2
1.5	10	8	3000	1.9×1.2

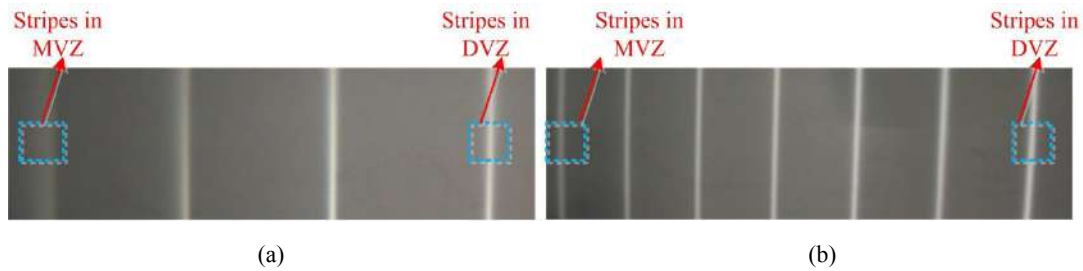


Fig 6. The light-field distribution in the viewing plane (a) $r = 5\text{mm}$ (b) $r = 10\text{mm}$

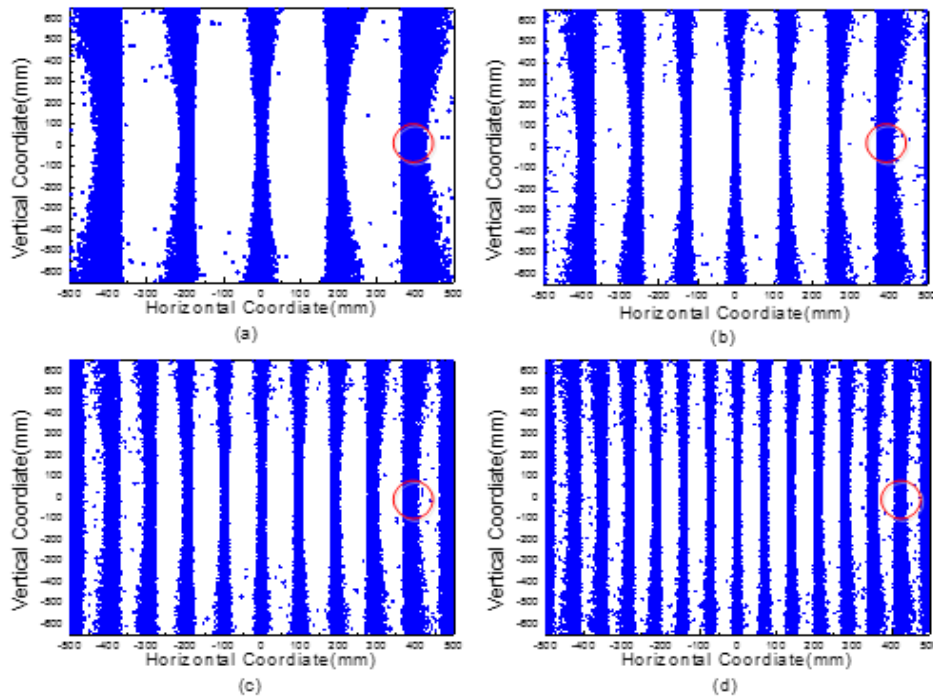


Fig 7. The distribution light-field with increasing ROC (a) $r = 4\text{ mm}$ (b) $r = 6\text{ mm}$ (c) $r = 8\text{ mm}$ (d) $r = 10\text{ mm}$

Figures 6(a) and 6(b) show the light-field distribution in the viewing plane of two lenticular sheets with different parameters. The distance of vertical stripes in the mid-viewing zone and the marginal viewing zone is 1350 mm, and the viewing angle of vertical stripes in the marginal viewing zone is $\arctan 1350/3000 \approx 24^\circ$. For Fig 6(b), the width of vertical stripes in the marginal viewing zone is close to the width of vertical stripes in the mid-viewing zone and they are both narrow, which means that the influences of aberration are small. When the arrangement of project or array is based on the light-field distribution on viewing plane in the mid-viewing zone, the overlapping part of adjacent viewpoints is little. According to the intensity measured from the adjacent overlapping part of the viewpoints in the viewing plane, the change of crosstalk degree can be obtained. Figure 7 shows the change of crosstalk degree along the horizontal coordinates. The range of horizontal coordinates is from 0 mm to 1350 mm. The crosstalk degree increase to 90% with $r = 5$ mm, and the change of the crosstalk is below 10% with $r = 10$ mm.



(a)

(b)

Fig 8(a). The final 3D image with $r = 5$ mmFig 8(b). The final 3D image with $r = 10$ mm

A projector array with 30 micro-projectors is used to project 30 parallax images on the two diffuse screens. Figure 8(a) and Fig 8(b) show the 3D images viewed in the marginal viewing zone based on two lenticular diffuse screens, respectively. The 3D image in Fig 8(a) includes blur and ghosts, where a high cross talk degree results in a low resolution and a decreasing of 3D depth. The 3D image ($1.9 \text{ m} \times 1.2 \text{ m}$) in Fig 8(b) with high quality in the mid-viewing zone and the marginal viewing zone is achieved, which shows that the aberration is suppressed. The 3Dclear depth of 1.5 m can be perceived.

Increasing ROC or decreasing aperture can suppress the aberration and provide 3D images with high quality. However, the FOV is decreased. As we know, when our eyes move from one viewing zone to another, a jump is noticed, which brings discomfort. Increasing FOV can reduce the frequency of the jump. It is necessary to have an excellent stereo vision without decreasing FOV. There is only one surface of lens cell can be alternative in the traditional lenticular sheet, and aberration can't be completely eliminated. To reduce the aberration, more variables should be added, such as dual-surface and a spherical surface. After the aberration is balanced, a satisfactory structure was designed. The parameters are shown in Table 2 and the structure is shown in Fig 9. The traditional cylindrical lens with $P = 1.5$ mm, $f = 10$ mm, $d = 1$ mm is used to compare with the novel structure. With the novel meniscus lens structure, the meridional vertical axis aberration is well suppressed, but it has not been eliminated completely.

Table 2. The designed parameters of lenticular sheet

P (mm)	r_1 (mm)	r_2 (mm)	k_1	k_2	f (mm)	d (mm)	n
1.500	1.710	2.040	0.274	2.267	10.000	1.000	1.5

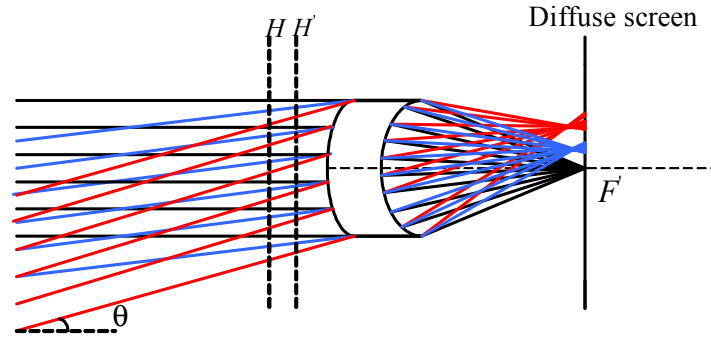


Fig 9. The actual meniscus thick lens

The distribution of light-field is shown in Fig 10. The corresponding normalized luminance distribution in the marginal viewing zone and the change of crosstalk degree in whole viewing angle are shown in Fig 11 and Fig 12.

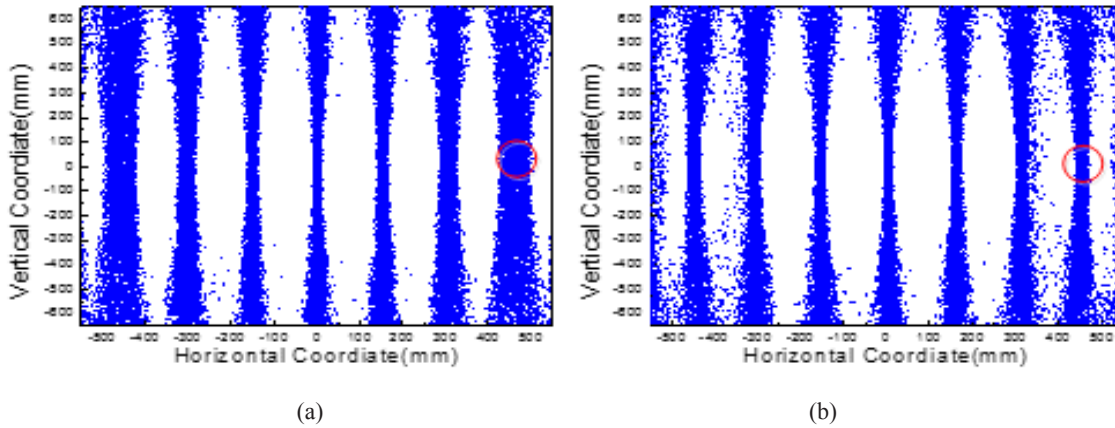


Fig 10. The distribution of light-field (a) The traditional lenticular sheet (b) The novel lenticular sheet

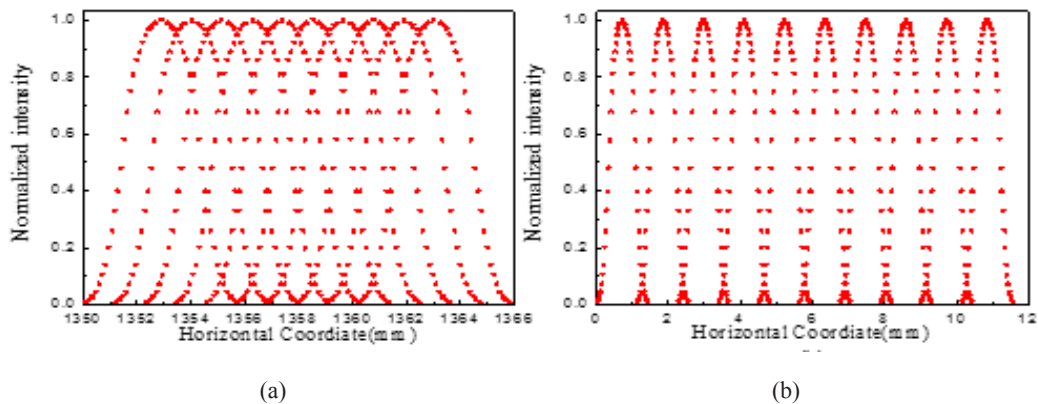


Fig 11. The normalized luminance distribution in MVZ (a) The traditional lenticular sheet (b) The novel lenticular sheet

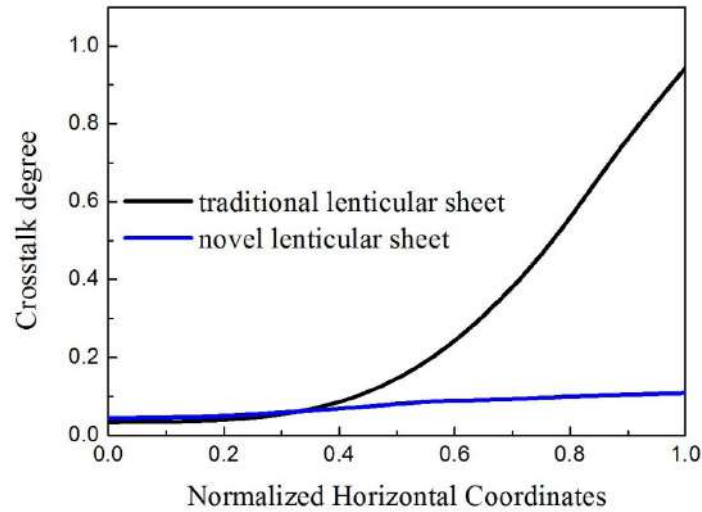


Fig 12. The change of crosstalk degree along the horizontal coordinates

The 3D display with a large bright fluctuation can lead to a perception discomfort. The configuration should be optimized to eliminate the abrupt brightness changes and to realize a smooth luminance perception [7]. The projector array is designed as shown in Fig 13. The middle view in a column w shows the highest luminance, and the luminance decreases one by one in both sides. The peaks of the brightness spectrum of light field fluctuate smoothly without any abrupt change. The Brightness fluctuation ration of the brightness spectrum is below 25%. The presented configuration method can present a better uniformity with the increasing of projectors.

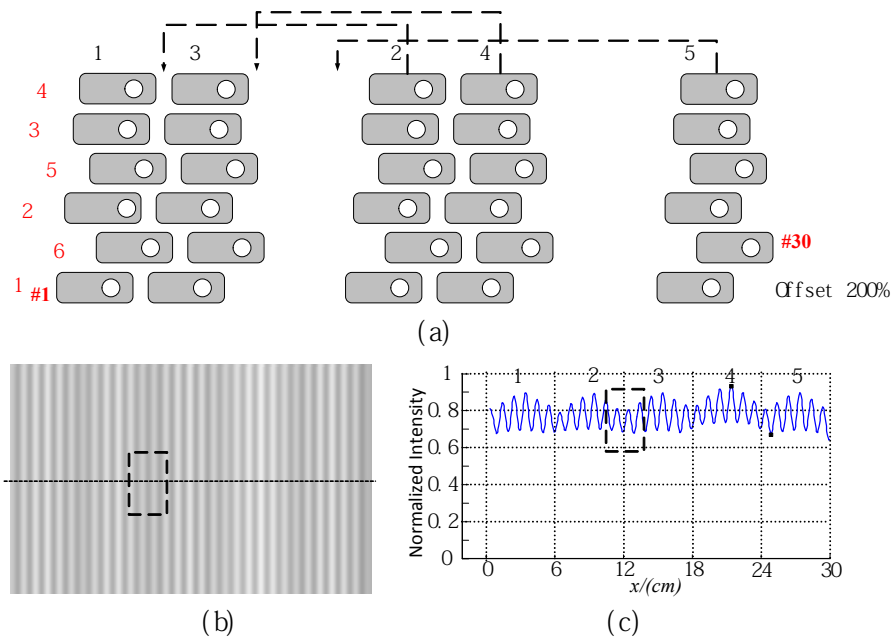


Fig 13. Optimized projector array with mixing rows.

The displayed depth of field (DOF) limitations of different lenticular-lens based 3D displays are shown in Fig 14. Left images show results of different displays with the same input scene with a DOF of (-368 mm, 467 mm), and right images show the cutoff frequency curve according to the displayed depth. Results of a normal lenticular-lens based LCD display with parameters of ($p = 0.4$ mm, $f = 5$ mm, $N_a = 8$) are shown in Fig 14(a). Figure 14(b) and Fig 14(c) show results of our proposed frontal projection 3D display with 18 projectors and 30 projectors, respectively. There is always a DOF limitation and a cutoff frequency in the 3D display system. When the displayed scene depth exceeds the DOF limitation, the cutoff frequency is decreased. The displayed scene blurs when the boundary of DOF is exceeded. Areas in the rectangles with red, blue and yellow colors show the scene in the front, middle and back sides, respectively. Compared with Fig 14(b) and (c), Fig 14(a) shows the worst image definition in the front and back sides of the scene. The 3D display with 30 projectors presents a maximum displayed depth of 590 mm, and the one with 18 projectors gives a DOF limitation of 350 mm. The depth of displayed scene is within the DOF limitation of 30-projector system, but some parts exceed the DOF limitation of the 18-projector one slightly. Results in Fig. 14 (b) show slight blur in the red and the blue rectangles, and results in Fig 14(c) show a good image definition.

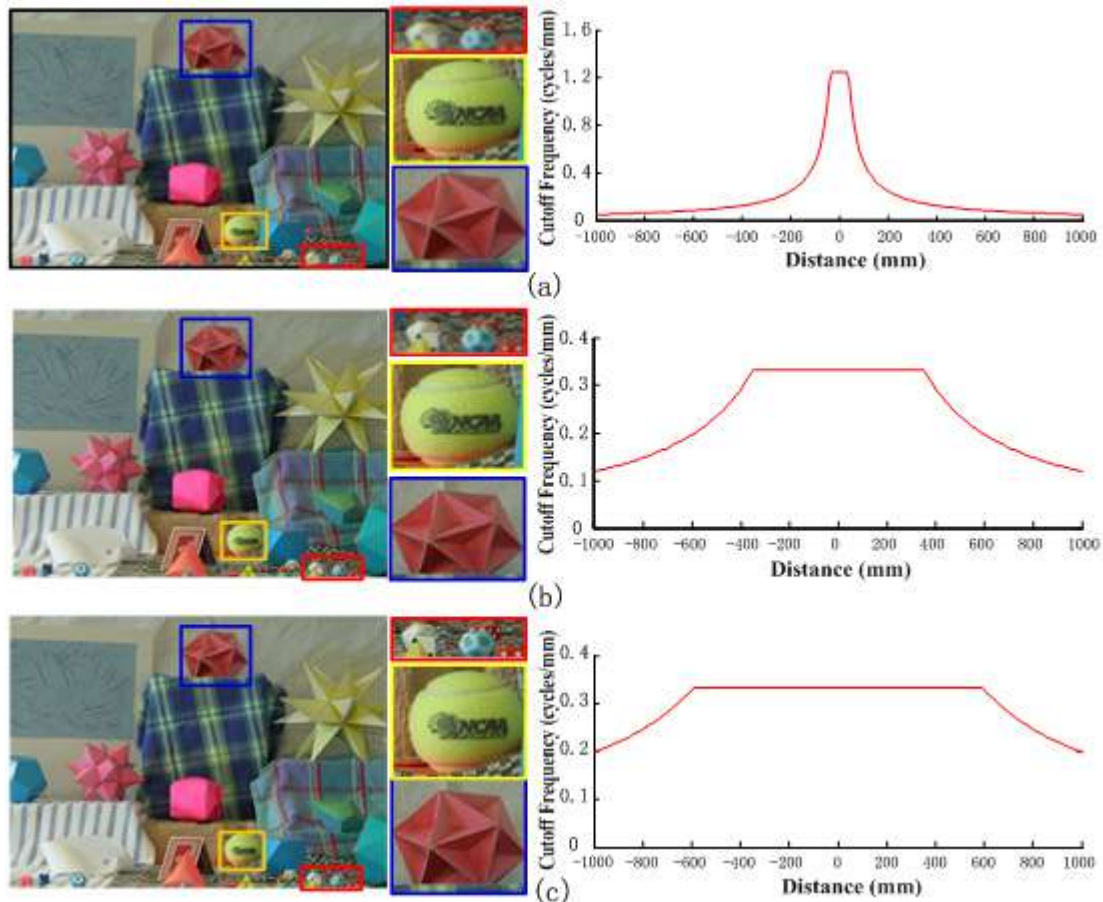


Fig 14. Results of different displays with the same scene. (a) Normal lenticular-lens based LCD display, (b) 3D display with 18 projectors, (c) 3D display with 30 projectors.

4 Conclusion

In summary, two large-size, high-resolution full-color project 3-D display systems based on the space multiplexing are demonstrated. The flexibility in terms of digitized recording and 3D diffuse screen based reconstruction relieves the limitations of conventional 3D display technologies while realizing fully continuous, natural 3-D display. The aberration of 3D diffuse screen is effectively suppressed and the crosstalk is well reduced.

Acknowledgments

This work is partly supported by the “863” Program (2012AA011902), the National Science Foundation of China (61177018), the Program for New Century Excellent Talents in University (NECT-11-0596), the fund of State Key Laboratory of Information Photonics and Optical Communications.

References

1. Moller C, Travis A, *Proc SPIE*, 5664(2005)150-157.
2. Xia X, Liu X, Li H, Zheng Z, Wang H, Peng Y, Shen W, *Opt Exp*, 21(2013)11237-11247.
3. Sang X, Fan F, Jiang C, Choi S, Dou W, Yu C, Xu D, *Opt Lett*, 34(2009)3803-3805.
4. Sang X, Fan F, Choi S, Jiang C, Yu C, Yan B, Dou W, *Opt Eng*, 50(2011)091303-1-5.
5. Benton S A, *Proc SPIE*, 367(1982)15-19.
6. Abookasis D, Rosen J, *J Opt Soc Am A*, 20(2003)1537-1545.
7. Wang P, Xie S, Sang X, Chen D, Li C, Gao X, Yu X, Yu C, Yan B, Dou W, Xiao L, *Opt Commun*, 354(2015)321-329

[Received : 17.10.2014]

Xinzhu Sang received dual bachelor's degrees in instrument science and management engineering from Tianjin University, Tianjin, China and the master's degree from Beijing Institute of Machinery, Beijing, China, in 1999 and 2002, respectively, and the Ph. D. degree in physical electronics at Beijing University of Posts and Telecommunications (BUPT), Beijing, China in 2005. Now he is with the BUPT as a Professor. His current research interests include novel photonic devices, optical communication, and 3-D display.



Binbin Yan received her bachelor's degree in electronic science and technology and the Ph. D degree in electromagnetic field and microwave technology from BUPT, Beijing, China, in 2003 and in 2010, respectively. Now she is a lecturer at BUPT. Her current research interests focus on photonic devices and optical communications.



Peng Wang received his bachelor's degree in Communication Engineering from University of Science & Technology Beijing, Beijing, China, in 2012. Now he is a Ph. D. student in State Key Laboratory of Information Photonics and Optical Communications, BUPT. His research interests include computational imaging, computational display and computer vision.



Xin Gao received his bachelor's degree in electronic information engineering from Chaohu University, Hefei, China, in 2012. He is currently a Ph. D. student in State Key Laboratory of Information Photonics and Optical Communications, BUPT. His research interests include optical system design and photolithography technique.



Gang-Ding Peng received B.Sc. in physics from Fudan University in 1982, and M.Sc in Applied Physics and Ph.D. in electronic engineering from Shanghai Jiao Tong University in 1984 and 1987, respectively. He has been working with UNSW, Australia since 1991. He is a fellow and life member of both OSA and SPIE. His research interests include Optical Fibres and devices, Fibre sensors and Nonlinear Optics.

